

https://dspace.org/

Vanadium Titanium and Iron Extraction from Titanomagnetite Ore by Salt Roasting and 21stCentury Solvents

Emmanuel Oke; Johannes Potgieter; David Nkhoesa; Lizelle Doreen Van Dyk

https://hdl.handle.net/10539/47371
WOS

Downloaded from a DSpace repository. https://dspace.org/

separations

IMPACT FACTOR 2.7

CITESCORE 4.5

Article

Vanadium, Titanium, and Iron Extraction from Titanomagnetite Ore by Salt Roasting and 21st-Century Solvents

Emmanuel Anuoluwapo Oke, Johannes Hermanus Potgieter, David Nkhoesa and Lizelle Doreen van Dyk

Special Issue

Advances in Separation and Leaching for Metal Recovery

Edited by

Dr. Yun Li and Dr. Hui Xu

MDPI

https://doi.org/10.3390/separations12100285

separations

MDPI

Article

Vanadium, Titanium, and Iron Extraction from Titanomagnetite Ore by Salt Roasting and 21st-Century Solvents

Emmanuel Anuoluwapo Oke, Johannes Hermanus Potgieter *, David Nkhoesa and Lizelle Doreen van Dyk

Sustainable and Innovative Minerals and Metals Extraction Technology (SIMMET) Research Group, School of Chemical and Metallurgical Engineering, University of the Witwatersrand, Private Bag X3 PO Wits 2050, Johannesburg 2050, South Africa

* Correspondence: herman.potgieter@wits.ac.za

Abstract

Vanadium is a strategic metal with critical applications in steel alloys, aerospace, chemical catalysis, and energy storage. However, conventional extraction methods such as high-temperature salt roasting are energy-intensive and environmentally challenging. This study investigated the extraction of V, Ti, and Fe from titanomagnetite ore using aqueous solutions of two ionic liquids (IL), 1-butyl-3-imidazolium hydrogen sulphate ([Bmim][HSO_4], and 1-butyl-3-methylimidazolium hexafluorophosphate [Bmim][PF_6]) as well as two deep eutectic solvents (DESs) (choline chloride:oxalic acid and choline chloride:succinic acid). Na_2CO_3 and Na_2SO_4 roasting were used as benchmarks for comparison purposes. Leaching was performed across a range of concentrations and temperatures, and metal recoveries were quantified by atomic absorption spectroscopy (AAS). Among all methods, ChCl:OA DES achieved the best leaching efficiencies of 97.6% for V, 76.1% for Ti, and 68.8% for Fe at 50% (*v*/*v*) and 100 °C, outperforming [Bmim][HSO_4] and conventional roasting. Kinetic analysis using the shrinking core model indicated that leaching is predominantly diffusion-controlled, with apparent activation energies of 35.1 kJ/mol for V, 28.3 kJ/mol for Ti, and 29.8 kJ/mol for Fe. The results demonstrate that ChCl:OA DES provides a low-temperature, biodegradable, and cost-effective approach for V, Ti and Fe extraction, offering a sustainable alternative to conventional salt roasting methods.

Keywords: deep eutectic solvent; ionic liquids; hydrometallurgy; kinetic modelling; activation energy

check for updates

Academic Editor: Guoquan Zhang

Received: 23 September 2025
Revised: 7 October 2025
Accepted: 11 October 2025
Published: 15 October 2025

Citation: Oke, E.A.; Potgieter, J.H.; Nkhoesa, D.; Dyk, L.D.v. Vanadium, Titanium, and Iron Extraction from Titanomagnetite Ore by Salt Roasting and 21st-Century Solvents. *Separations* **2025**, *12*, 285. https://doi.org/10.3390/separations12100285

Copyright: © 2025 by the authors. Licensee MDPI, Basel, Switzerland. This article is an open access article distributed under the terms and conditions of the Creative Commons Attribution (CC BY) license (https://creativecommons.org/licenses/by/4.0/).

1. Introduction

Vanadium is a rare and strategically important metal, valued primarily for its unique properties in both ferrous and non-ferrous alloy production [1]. With ongoing advancements in science, technology, and the economy, global demand for vanadium is projected to rise significantly [2,3]. Owing to its wide-ranging applications and the steady growth in its consumption, vanadium extraction has become an area of notable interest. Currently, vanadium is valued at approximately USD 20,000–40,000 per metric ton [4]. Vanadium occurs in a variety of minerals and is the 22nd most common element in the Earth's crust [5]. Despite the relatively large global reserves, most vanadium resources are scattered and occur chiefly as symbiotic or composite ores, with no significant deposits of vanadium existing in isolation [6]. Many undesirable impurities like Fe, Mg, and Al exist alongside vanadium in its ores [7]. The main primary sources of vanadium are typically divided into three groups: vanadium titanomagnetite, shale-hosted deposits, and sandstone-hosted

vanadium deposits [5]. Currently, nearly 88% of the world's vanadium resources are obtained from vanadium titanomagnetite, while most of the remainder is sourced from vanadium-bearing stone coal [8]. Major vanadium reserves are concentrated in a few countries, notably China (36.8%), South Africa (31.6%), Russia (18.4%), and the United States (10.5%), with other nations holding less than 3.0% collectively [9]. In China, over 87.0% of vanadium resources exist in vanadium shale, making extraction from this source particularly critical [10].

Vanadium's strategic significance spans several industries, including steel manufacturing, aerospace, chemical processing, and energy storage [8,11]. In metallurgy, trace additions of vanadium enhance steel's strength, toughness, ductility, and heat resistance [12]. The aerospace sector utilises vanadium-titanium-aluminium alloys to produce components such as missile casings, nuclear reactor parts, jet engines, and airframes [8,9]. Chemically, vanadium serves as a catalyst, particularly in the production of sulfuric acid [13]. In energy storage, vanadium pentoxide (V_2O_5) is a key material for electrolytes in vanadium redox flow batteries, which are recognised for their long lifespan, safety, efficiency, and environmental compatibility [14,15]. Beyond these, vanadium finds applications in thin films, pharmaceuticals, and emerging high-tech materials such as nanostructures and films [8,16,17]. Recognised as an essential national strategic resource, vanadium has been likened to the "monosodium glutamate of modern industry" due to its indispensable role in industrial development [18,19]. Its primary application remains in the manufacture of vanadium steels known for their superior mechanical properties, including high strength and wear resistance [20]. The expanding range of applications, from aerospace alloys to catalytic processes and advanced battery technologies, underscores the urgent need for efficient utilisation of vanadium resources [18,21].

The salt roasting method remains the predominant industrial method for extracting vanadium from sources like titanomagnetite ores or spent catalysts. It involves mixing the vanadium-bearing material with sodium additives (typically Na_2CO_3, NaCl, NaOH or Na_2SO_4, 5–20 wt.%) and roasting at 750–900 °C in air [8,18]. This oxidises vanadium and converts it into water-soluble sodium vanadates (e.g., $NaVO_3$). Subsequent water leaching dissolves the vanadates, separating them from the insoluble residue for further purification and precipitation [4,11]. The leaching efficiency of vanadium using this method could reach 79.1% and 91.0% [22,23]. Despite its effectiveness, the process faces challenges, including high energy consumption and the generation of corrosive gases (HCl, Cl_2, SO_2, and SO_3, among others), especially when using chloride or sulphate additives, driving research into cleaner alternatives [24,25]. These gases facilitate the structural breakdown of minerals and promote further oxidation, but they can also pose significant environmental pollution risks [26].

While pyrometallurgical processing of vanadium-titanium magnetite is still being optimised for low-carbon and efficient reduction routes [27,28]. The urgent global trend is toward sustainable, mild hydrometallurgical alternatives. Recent advances have focused on enhancing extraction kinetics using techniques like microwave-assisted leaching [29] and pioneering low-temperature bioleaching methods, which have achieved significant vanadium recovery under environmentally benign conditions [30]. Critically, research has highlighted that the high leaching efficiency of vanadium in these mild processes is often directly attributed to the strong chelating and lixiviating capability of organic acids, particularly oxalic acid [31]. This growing evidence for mild, organic-acid-driven extraction mechanisms provides a compelling scientific rationale for utilising oxalic acid as a key component in 21st-century solvents for complex ore processing.

In recent years, ionic liquids (ILs) and deep eutectic solvents (DESs) have emerged as highly promising green leaching alternatives, largely due to their relatively low toxicity

and minimal environmental impact. Their application as solvents and reagents in mineral processing and the extraction of valuable elements offers a viable substitute for conventional metallurgical and mineral processing methods, thereby advancing cleaner and more sustainable production practices [32]. ILs possess a range of unique properties, including low melting points, negligible vapour pressure, high thermal stability, wide electrochemical windows, and excellent solubility for diverse substances [33]. They are non-flammable, recyclable, and environmentally benign, making them valuable green solvents. Owing to their tunable nature, ILs have found wide application in fields such as catalysis, material synthesis, separation processes, electrochemistry, and energy storage technologies [34]. Only a few studies have employed ILs for the extraction of vanadium. For instance, Luo et al. developed an efficient method to recover vanadium from vanadium shale leach solutions using the ionic liquid tri-n-octylmethylammonium chloride (TOMAC) [7]. Under optimised conditions, a three-stage extraction achieved 98.1% vanadium recovery [7]. Also, in 2024, Yu et al. reported that vanadium could be efficiently extracted from sulphuric acid shale leachate using TOMAC, achieving 90.5% recovery in a single-stage extraction under optimised conditions [35]. Additionally, Potgieter and Teimouri proposed a green approach for extracting vanadium from slag using the ionic liquids 1-butyl-3-methylimidazolium trifluoromethane sulfonate, [BmimCF_3SO_3], and 1-butyl-3-methylimidazolium hydrogen sulphate, [BmimHSO_4]. Under optimised conditions with [BmimHSO_4], they achieved a maximum vanadium recovery of 94.2% from the non-magnetic slag fraction [36]. Recently, salicylhydroxamic acid, TOMAC, and tributyl phosphate in sulfonated kerosene were used as a bifunctional extraction method for purifying and enriching vanadium from direct acid leachates of V-bearing shale without pH adjustment. Under optimised conditions, the system achieved 84.9% vanadium recovery in the first stage [37].

DESs are a new type of solvent made by mixing two or more components (i.e., hydrogen bond donor and hydrogen bond acceptor) that form a liquid with a melting point lower than that of each component [38]. They are similar to ILs but are easier to prepare, less toxic, and more environmentally friendly [39]. DESs are often made from natural substances and have versatile uses, including pharmaceutical formulation, metal extraction, catalysis, organic synthesis, biomass processing, and environmental remediation [40,41]. Their unique properties come from strong hydrogen bonding, which lowers the melting point and allows them to dissolve many analytes effectively. These features make DESs a promising green alternative to traditional solvents. To date, the application of DESs in the extraction of vanadium remains very limited. The only published work in this area was carried out by Surauzhanov and Ultarakova, who investigated the leaching of vanadium from the dust of ore-thermal melting using DESs prepared from choline chloride and various carboxylic acids [42]. Their results demonstrated that the oxaline system was particularly effective, achieving a vanadium recovery of 89.0%.

In this study, titanomagnetite vanadium ore from a newly developed mine in Mpumalanga, South Africa, was processed using three distinct approaches: salt roasting, ILs and DESs. The ILs [Bmim][HSO_4] and 1-butyl-3-methylimidazolium hexafluorophosphate ([Bmim][PF_6]), were selected for their thermal stability, high solubility and environmental compatibility. The DESs used in this study were prepared using choline chloride (ChCl) as the hydrogen bond acceptor (HBA), succinic acid (SA) and oxalic acid (OA) as hydrogen bond donors (HBDs). SA is a biodegradable, renewable, low-toxicity organic acid that is inexpensive and non-toxic [43]. OA, in contrast, offers stronger acidity and a more effective hydrogen bond donation capacity due to its carboxylate groups [44]. ChCl is an affordable compound widely used in animal husbandry [43]. Sodium carbonate (Na_2CO_3) and sodium sulphate (Na_2SO_4) were used for conventional salt roasting as a reference. The novelty of this work lies in the first reported application of these specific

aqueous solutions of ILs and DESs for vanadium extraction from titanomagnetite ore, with a systematic comparison to conventional salt roasting, providing new insights into sustainable and efficient extraction strategies.

2. Materials and Methods

2.1. Chemicals

Titanomagnetite vanadium ore was sourced from a newly developed mine in Mpumalanga, South Africa. Oxalic acid dihydrate (OA, ≥99.5%, CAS No. 6153-56-6), succinic acid (SA, ≥99.0%, CAS No. 110-15-6), 1-butyl-3-imidazolium hydrogen sulphate ([Bmim][HSO_4], ≥95%, CAS No. 262297-13-2), 1-butyl-3-methylimidazolium hexafluorophosphate ([Bmim][PF_6], ≥98.5%, CAS No. 174501-64-5), sodium carbonate (Na_2CO_3, ≥99.5%, CAS No. 497-19-8), and sodium sulphate (Na_2SO_4, ≥99.5%, CAS No. 7757-82-6) were all purchased from Sigma-Aldrich (St. Louis, MO, USA). All chemicals were used without any further purification, and deionised water was employed in solution preparation.

2.2. Collection of Sample and Preparation

In this study, a representative titanomagnetite vanadium ore sample was collected from a newly developed mine in Mpumalanga, South Africa. Approximately 5 kg of the ore was homogenised through thorough blending to ensure sample uniformity and representativeness. The material was subsequently reduced in size using a ball mill followed by a pulveriser, after which it was sieved through a 75 μm sieve to obtain the desired particle fraction.

2.3. Characterisation of Sample

The representative titanomagnetite ore sample obtained with a size fraction of 75 μm was characterised using several analytical techniques. The overall chemical composition was determined by X-ray fluorescence (XRF), Bruker S2 Ranger (Bruker, Billerica, MA, USA), operated at a tube voltage of 60 kV and a tube current of 40 μA. The results are presented in Table 1. The crystalline phases were identified by X-ray diffraction (XRD), Bruker D2 Phaser (Bruker, Karlsruhe, Germany), using Co-Kα radiation (λ = 1.8 Å), operated at 50 kV and 25 mA, with scans recorded over the 2θ range of 10–90° for 10 min. Both pre-leached and post-leached samples were characterised by XRD to assess the phase changes resulting from the leaching process.

Table 1. Chemical composition of the titanomagnetite ore as determined by XRF.

Composition	Na_2O	MgO	Al_2O_3	SiO_2	SO_3	K_2O	CaO	TiO_2	V_2O_5	MnO	Fe_2O_3	CuO
Mass %	1.20	2.10	17.10	39.8	0.23	0.20	11.80	3.00	0.56	0.21	23.50	0.13

2.4. Synthesis of the DESs

In this study, two carboxyl-based DESs were prepared using ChCl as the HBA and OA or SA as the HBDs. The mixture of ChCl and the respective HBD in a 1:1 molar ratio was heated in an oil bath at 80 °C, with continuous stirring until a homogeneous, transparent liquid was obtained. The resulting DESs, ChCl:OA and ChCl:SA, were previously reported [38,45]. After synthesis, the DESs were allowed to cool to room temperature, vacuum-dried at 65 °C for 24 h, and stored in a desiccator for 5 days to prevent moisture absorption before use. Additionally, two ILs, [Bmim][HSO_4] and [Bmim][PF_6], were employed in this work, and their chemical structures are shown in Figure 1 alongside those of the HBA and HBD used for the DESs synthesis.

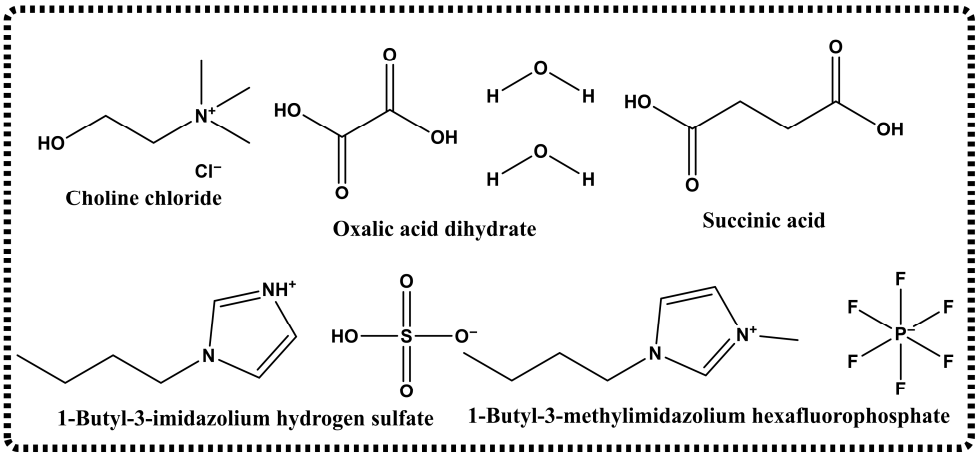


Figure 1. Chemical structures of ILs and DES components used in this study.

2.5. Extraction Procedures

2.5.1. Roasting with Salts

Two sodium salts, Na_2CO_3 and Na_2SO_4, were investigated for roasting the titanomagnetite ore sample. The effect of salt dosage and roasting temperature was studied by varying salt additions between 5% and 25% (*w*/*w*) and applying furnace temperatures from 600 °C to 850 °C for 90 min. The roasted products were subsequently subjected to water leaching. In each case, 10 mL of deionised water was added to 1 g of roasted sample to achieve a liquid-to-solid ratio of 10:1 (mL/g).

2.5.2. Leaching with ILs and DESs

Leaching experiments were conducted in a three-necked round-bottom flask coupled to a reflux condenser, with temperature controlled by an oil bath and agitation maintained using a magnetic stirrer. Four solvents were investigated for metal extraction: two ILs ([Bmim][HSO_4] and [Bmim][PF_6]) and two DESs (ChCl:OA and ChCl:SA). Solutions (20–60% *v*/*v*) of different concentrations were prepared by dilution with deionised water, and 10 mL of each solution was added to 1 g of ore (liquid-to-solid ratio 10:1 mL/g). Leaching was performed at 80 °C for 90 min under continuous stirring at 250 rpm. After leaching, solid–liquid separation was achieved using a Whatman No. 42 filter fitted into a Büchner funnel connected to a filtration pump, and the residue was thoroughly washed with 40% ethanol to remove residual solvent and impurities. Aliquots (1 mL) of the leachates were diluted to 100 mL with deionised water in standard volumetric flasks, and metal concentrations were determined by atomic absorption spectroscopy (AAS, Agilent 200 series). Leaching efficiency (LE, %) was calculated according to Equation (1).

$$\mathrm{LE} = \frac{C_0}{C_i} \times 100\% \quad (1)$$

In the equation above, C_o denotes the concentration of metal in the filtrate, while C_i represents the concentration of metal in the original sample. All experiments were conducted in duplicate, and average values are reported.

The liquid-to-solid (L/S) ratio was fixed at 10 mL/g (10:1) for all leaching experiments. This ratio was selected as a necessary compromise between achieving optimal chemical kinetics and maintaining high industrial feasibility. A lower ratio (high pulp density) significantly increases the pulp viscosity, which is a major concern with ILs and DESs, enhancing mass transfer resistance and restricting the diffusion of the lixiviant to the reaction interface [46]. Conversely, while higher ratios minimise diffusion control and thus maximise the reaction rate, they are inefficient and unsustainable due to the increased volume of

solvent required, leading to high reagent consumption, higher energy costs for heating, and substantial increases in downstream solvent recovery costs [47]. The 10 mL/g ratio provided the required solvent volume for effective leaching while minimising operational costs. The roasting time was fixed at 90 min (1.5 h) based on the previous studies. This time is sufficient for the high-temperature solid-state conversion of vanadium-bearing species into soluble vanadates to approach completion [23]. Critically, prolonging the roasting time beyond this point is counterproductive because the extended exposure promotes thermal sintering of the ore, which forms a dense, restrictive layer. This layer encapsulates the converted vanadium compounds, thereby drastically reducing the accessibility of the lixiviant and causing a detrimental drop in leaching efficiency [48,49].

3. Results and Discussion

3.1. Roasting with Sodium Salts

The roasting of vanadium-bearing titanomagnetite ore with sodium salts significantly affected the leaching efficiencies of V, Ti, and Fe. When Na_2CO_3 was employed, V recovery increased with salt dosage, reaching 86.5% at 20 wt.%, while Ti and Fe reached 50.6% and 66.6%, respectively (Figure 2a). Increasing Na_2CO_3 to 25 wt.% caused a slight decline in recoveries of the metals investigated (V = 82.2%, Ti = 49.2%, and Fe = 64.2%). The enhanced V extraction when the salt dosage was increased from 5 wt.% to 20 wt.% could be primarily due to the formation of water-soluble sodium vanadates. During roasting, vanadium pentoxide (V_2O_5) reacts with sodium carbonate to form sodium metavanadate ($NaVO_3$) and sodium orthovanadate (Na_3VO_4) according to the reactions below:

$$V_2O_5 + Na_2CO_3 \rightarrow 2NaVO_3 \text{ (sodium metavanadate)} + CO_2 \quad (2)$$

$$V_2O_5 + 3Na_2CO_3 \rightarrow 2Na_3VO_4 \text{ (sodium orthovanadate)} + 3CO_2 \quad (3)$$

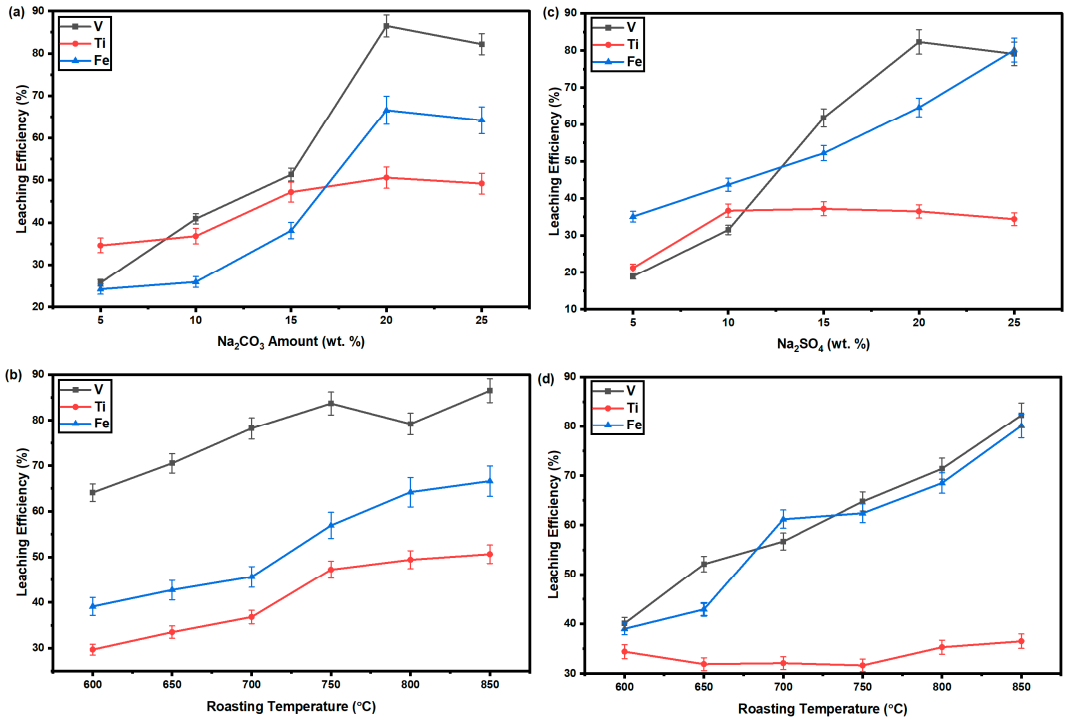


Figure 2. (**a**) Effect of Na_2CO_3 amount (90 min, 850 °C); (**b**) Effect of roasting temperature using Na_2CO_3; (**c**) Effect of Na_2SO_4 amount (90 min, 850 °C); (**d**) Effect of roasting temperature using Na_2SO_4 on the roasting of titanomagnetite vanadium ore sample [leaching temperature of 25 °C, stirring speed of 250 rpm, duration of 90 min and a liquid-to-solid ratio of 10:1 (mL/g)].

At lower Na_2CO_3 dosages (<15 wt.%), incomplete conversion of vanadium oxides limited soluble vanadate formation, reducing leaching efficiency. Conversely, excessive Na_2CO_3 (>20 wt.%) may react with silicates or aluminates in the ore to form undesired byproducts, such as sodium silicates or aluminates, which hinder V extraction [26,50].

Roasting temperature also played a critical role. At 20 wt.% Na_2CO_3, leaching efficiencies of V, Ti, and Fe increased with temperature, reaching their highest at 850 °C (V = 86.5%, Ti = 50.6%, Fe = 66.6%) as depicted in Figure 2b. This implies that lower temperatures (<800 °C) were insufficient to fully oxidise V^{3+}/V^{4+} to the more soluble V^{5+}, limiting sodium vanadate formation. The oxidation of V_2O_3 to V_2O_5 can be represented as:

$$V_2O_3 + O_2 \rightarrow V_2O_5 \quad (4)$$

Roasting with Na_2SO_4 displayed similar trends, though V and Ti recoveries were slightly lower. V recovery increased from 5 to 20 wt.% Na_2SO_4, reaching 82.5%, then declined to 79.1% at 25 wt.% (Figure 2c). Ti recovery remained relatively constant (ranging between 21.2% and 37.2%), while Fe increased from 35.1% at 5 wt.% Na_2SO_4 to 80.1% at 25 wt.% Na_2SO_4. Unlike Na_2CO_3, Na_2SO_4 does not directly react to form soluble vanadates but acts as a flux, promoting diffusion of V_2O_5 and partial vanadate formation at elevated temperatures [51]. Excess Na_2SO_4 functions as an inert diluent, reducing effective contact with vanadium oxides and lowering extraction efficiency.

The effect of roasting temperature with Na_2SO_4 indicated that V and Fe leaching increased with temperature (Figure 2d). For instance, the leaching efficiency of V increased from 40.1% at 600 °C, and it reached the highest level (82.3%) at 850 °C. Also, Fe leaching efficiency increased from 39.0% at 600 °C and reached the greatest efficiency of 80.1% at 850 °C. However, the leaching efficiency of Ti was observed to be low, ranging between 31.6% and 36.5% throughout the studied temperatures.

The leaching efficiency reached a maximum at 850 °C, leading to the highest vanadium recovery, while Ti and Fe recoveries remained modest. Although 850 °C did not fully optimise extraction for all elements, we deliberately limited our investigation to this maximum. This decision was based on the confirmed phenomenon of thermal sintering in titanomagnetite ores at higher temperatures, which negatively impacts metal accessibility. In preliminary testing, a higher temperature of 900 °C was also evaluated, but the observed vanadium recovery was lower than at 850 °C. This outcome aligns with previous reports that temperatures above 900 °C do not further enhance leaching due to increased sintering and reduced accessibility of the target elements within the ore [52]. Consequently, 850 °C represents the critical thermal peak before detrimental effects dominate the process.

In summary, Na_2CO_3 outperformed Na_2SO_4 for V and Ti extraction, while Fe recovery was found to be similar. The superior performance of Na_2CO_3 could be due to its stronger alkalinity, fluxing properties, and rapid reaction with vanadium oxides, which promotes the formation of soluble vanadates [26,51]. Lower leaching efficiencies obtained when Na_2SO_4 was used for the recovery of V are likely due to the formation of sulphate-containing byproducts that can interfere with V extraction. In summary, 20 wt.% Na_2CO_3 at 850 °C for 90 min represents the optimal roasting condition for efficient V, Ti and Fe recovery.

3.2. Leaching with ILs

The performance of ionic liquid leaching was investigated using [Bmim][HSO_4] and [Bmim][PF_6]. Both systems were assessed for the effect of concentration, while only [Bmim][HSO_4] was further examined for the effect of temperature due to its superior leaching efficiency. These parameters influence dissolution kinetics by altering solubility, diffusion, and mass transfer from the solid sample into the IL.

3.2.1. Effect of Varying IL Concentration

The dissolution behaviour of the titanomagnetite ore sample was studied across an IL concentration range spanning 20 to 60 v/v% using [Bmim][HSO_4] and [Bmim][PF_6] ILs. Figure 3a,b illustrate the effect of IL concentration on the leaching efficiencies of V, Ti, and Fe using [Bmim][HSO_4] and [Bmim][PF6], respectively. In both systems, the general trend shows an improvement in metal leaching efficiencies as the IL concentration increases, consistent with previous studies that reported higher extraction efficiencies at elevated IL concentrations [53,54]. For [Bmim][HSO_4] (Figure 3a), the highest leaching performance was obtained at 50% (v/v), with efficiencies of 86.7% for V, 67.3% for Fe, and 42.7% for Ti. A sharp increase in V leaching was observed between 40% and 50% (v/v), rising from 58.7% to 86.7%, but the efficiency subsequently declined to 77.1% at 60% (v/v), likely due to the high viscosity of IL-rich solutions, which hindered mass transfer. Similarly, Fe extraction decreased slightly from 67.3% to 66.7% when the concentration was raised from 50% to 60% (v/v). Ti, however, continued to increase progressively across the studied range, from 24.5% to 42.7%.

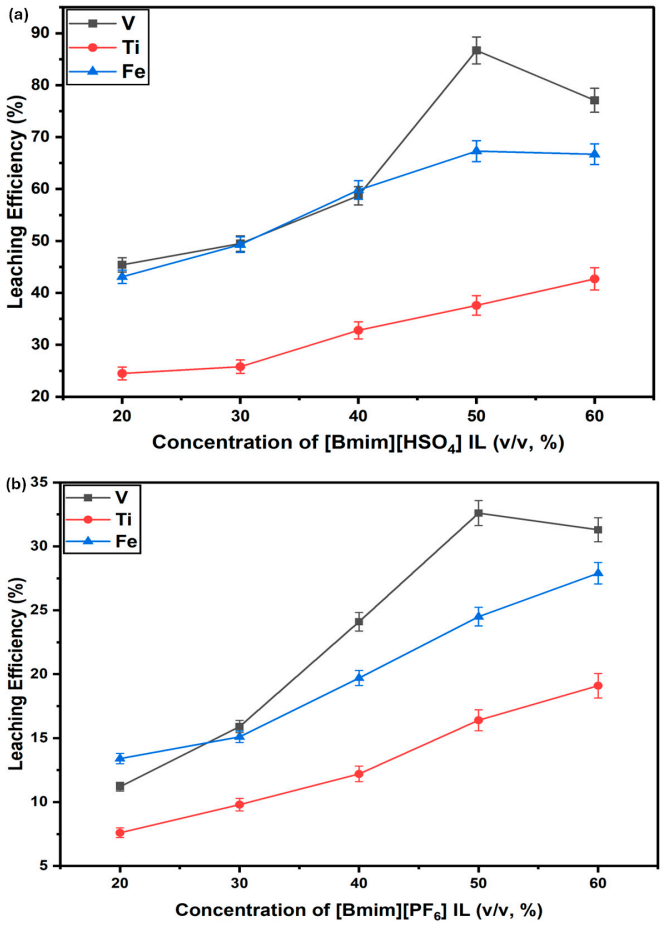


Figure 3. Effect of concentrations of different ILs (**a**) [Bmim][HSO_4]; and (**b**) [Bmim][PF_6] [leaching temperature = 80 °C, liquid-to-solid ratio = 10:1 (mL/g), stirring speed = 250 rpm and leaching time= 90 min].

For [Bmim][PF_6] (Figure 3b), leaching efficiencies were lower overall compared to [Bmim][HSO_4]. The maximum efficiencies at 50% (v/v) were 32.6% for V, 24.5% for Fe, and 16.4% for Ti. At 60% (v/v), V extraction declined slightly to 31.3%, and Ti increased modestly to 19.1%, while Fe continued to rise to 27.9%. These results suggest that [Bmim][HSO_4] offers superior leaching performance compared to [Bmim][PF_6], likely due to its acidic nature, which enhances metal dissolution, whereas [Bmim][PF_6] is more hydrophobic and

less effective as a leaching medium. The observed trend can be explained mechanistically. [Bmim][HSO_4] dissociates in solution to release protons that attack the oxide lattices. The proposed chemical reactions for the leaching of the investigated metals using [Bmim][HSO_4] IL are shown in Equations (5)–(8) according to the previous studies [36,54,55]. Since 50% (*v*/*v*) concentration of [Bmim][HSO_4] IL demonstrated the best performance, it was employed for further experiments.

$$[Bmim][HSO_4]_{(l)} \leftrightarrow [Bmim]^+_{(aq.)} + H^+_{(aq.)} + SO_4{}^-_{(aq.)} \quad (5)$$

$$V_2O_{5(s)} + 2H^+_{(aq.)} \rightarrow 2VO_2{}^+_{(aq.)} + H_2O_{(l)} \quad (6)$$

$$TiO_{2(s)} + 4H^+_{(aq.)} \rightarrow Ti^{4+}_{(aq.)} + 2H_2O_{(l)} \quad (7)$$

$$Fe_2O_{3(s)} + 6H^+_{(aq.)} \rightarrow 2Fe^{3+}_{(aq.)} + 3H_2O_{(l)} \quad (8)$$

3.2.2. Effect of Varying Temperature

The influence of temperature on metal leaching was examined using a 50% (*v*/*v*) [Bmim][HSO_4] at a liquid-to-solid ratio of 10 mL/g for 90 min (Figure 4). The leaching efficiencies of V, Ti, and Fe all improved with rising temperature. At 20 °C, the efficiencies were relatively low (49.8% V, 27.1% Ti, and 28.2% Fe), but steadily increased with temperature, reaching 95.6% V, 53.2% Ti, and 74.8% Fe at 100 °C. This positive correlation between temperature and leaching performance can be attributed to several factors: (i) enhanced solubility of metals in the IL medium at higher temperatures, allowing greater dissolution into the liquid phase; (ii) enhanced diffusion due to increased particle mobility, which accelerates mass transfer from solid to liquid; and (iii) reduced viscosity of the IL at elevated temperatures, which facilitates better transport of dissolved species. [39,56]. Among the metals studied, V was the most responsive to temperature, showing a marked increase from 70.2% at 60 °C to 95.6% at 100 °C. Fe extraction also benefited significantly, rising from 44.5% to 74.8% over the same range. Ti, however, showed consistently lower dissolution efficiencies (27.1–53.2%), which could be linked to the slower dissolution kinetics of titanium-bearing phases such as magnesium–titanium oxide ($MgTiO_3$), known to limit the solubility of Ti in IL media [57].

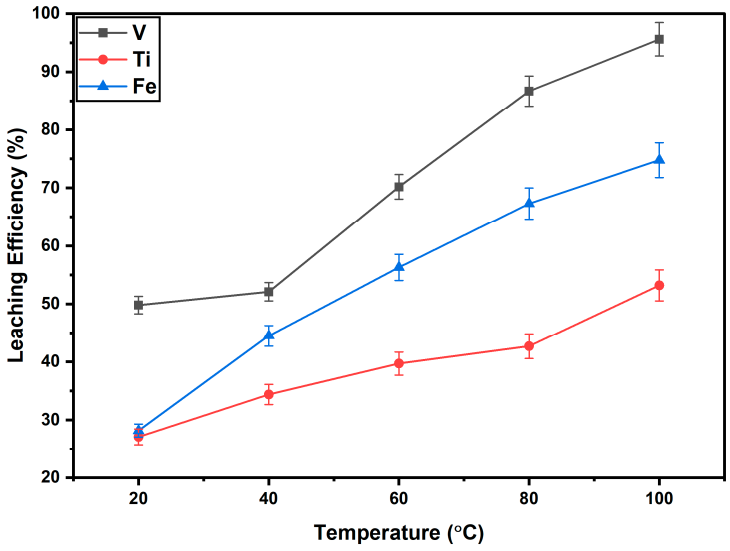


Figure 4. Effect of varying temperature on the leaching of the investigated metals using IL [IL = 50% *v*/*v* [BminSO_4], time = 90 min, stirring speed = 250 rpm, and liquid-to-solid ratio = 1/10 (mL/g)].

3.3. Leaching with DESs

The leaching performance of the investigated metals was investigated using ChCl:OA) and ChCl:SA. Both systems were evaluated for the effect of concentration, while only ChCl:OA was further examined for the effect of temperature since it demonstrated superior leaching performance for V.

3.3.1. Effect of Varying DES Concentration

Figure 5a,b depicts the effect of DES concentration on the leaching efficiencies of V, Ti, and Fe using ChCl:OA) and ChCl:SA, respectively. In both DES systems, an increase in concentration from 20% to 60% (v/v) generally resulted in enhanced metal leaching efficiencies, aligning with findings from previous studies that observed improved extraction efficiencies at elevated DES concentrations. For ChCl:OA leaching platform (Figure 5a), leaching efficiencies increased significantly across the concentration range. For instance, V extraction rose from 54.9% at 20% (v/v) to a maximum of 88.5% at 50% (v/v), with a slight decline to 87.2% at 60% (v/v). Also, Ti leaching showed a steady increase from 34.1% to 64.2%, while Fe extraction also improved from 29.3% to 53.7% over the same range. The slight decrease in V extraction at the highest concentration may be attributed to increased viscosity of the DES-rich solution, which can hinder mass transfer and slow the diffusion of dissolved metal ions.

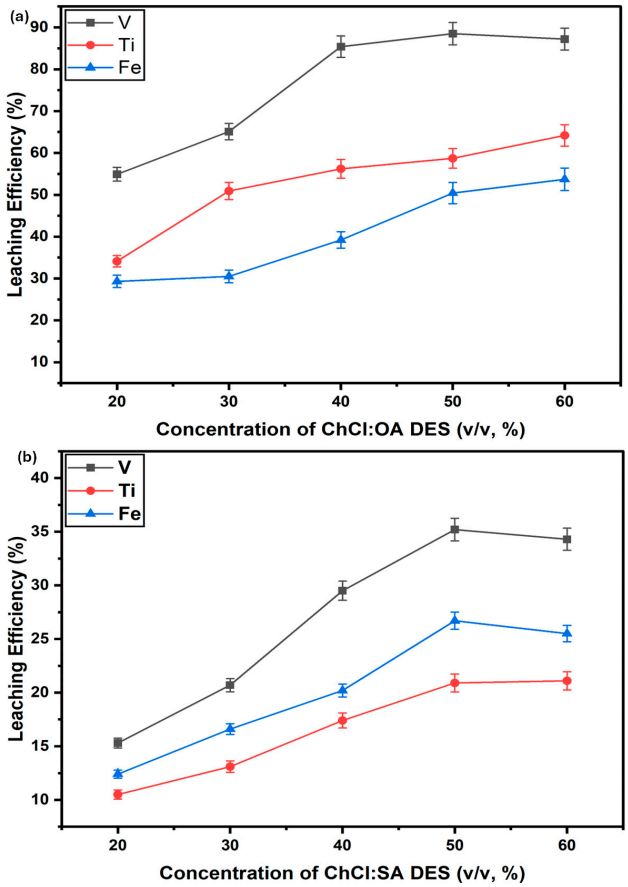


Figure 5. Effect of concentrations of different ILs (**a**) ChCl:OA; and (**b**) ChCl:SA [leaching temperature = 80 °C, liquid-to-solid ratio = 10:1 (mL/g), stirring speed = 250 rpm and leaching time = 90 min].

In contrast, the ChCl:SA leaching system (Figure 5b) demonstrated lower overall leaching efficiencies for all three metals. In this case, V extraction increased from 15.3% at 20% (v/v) to 35.2% at 50% (v/v) but slightly declined to 34.3% at 60% (v/v). In addition, Ti and Fe

showed gradual increases, reaching 21.1% and 25.5%, respectively, at the highest concentration. These results indicate that the oxalic acid-based DES (ChCl:OA) is significantly more effective than the succinic acid-based DES (ChCl:SA), likely due to its stronger acidity and ability to form stable metal–ligand complexes, which facilitate selective dissolution [42,43]. Previous studies further support the superior efficiency of the ChCl:OA DES solution, demonstrating that the solubility of metal oxides is greater in DESs containing oxalic acid [43,45,58]. Overall, ChCl:OA at 50% (v/v) provided the optimal leaching performance for V, Ti, and Fe and was therefore chosen for further temperature-dependent studies.

3.3.2. Effect of Varying Temperature

The effect of temperature on the leaching efficiencies of V, Ti, and Fe from a titanomagnetite ore using a 50% (v/v) ChCl:OA DES is presented in Figure 6. The leaching process was conducted under controlled conditions: 1 g of ore was mixed with 10 mL of the DES, maintaining a solid-to-liquid ratio of 1:10, and the mixture was heated on a magnetic hot plate for 90 min, with temperatures increasing from 20 °C to 100 °C in 20 °C increments. The results demonstrate a significant positive correlation between temperature and leaching efficiency for all three metals. At 20 °C, the leaching efficiencies were 27.5% for V, 25.0% for Ti, and 18.8% for Fe. As the temperature increased to 100 °C, the efficiencies rose to 97.6% for V, 76.1% for Ti, and 68.8% for Fe. This trend is consistent with chemical kinetics principles, where elevated temperatures enhance the kinetic energy of molecules, promoting more frequent and effective collisions between the DES and ore particles [59,60].

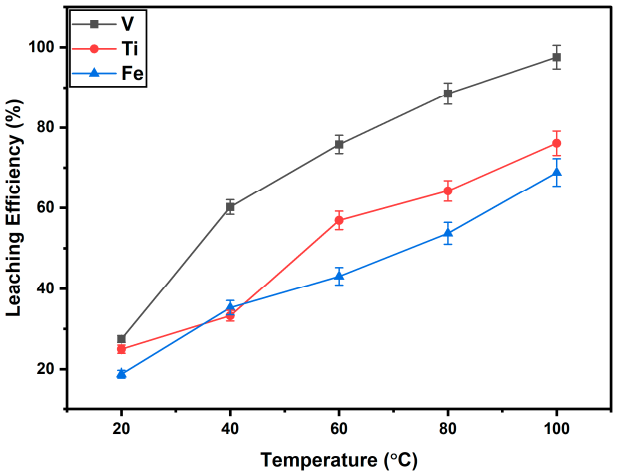


Figure 6. Effect of varying temperature on the leaching of the investigated metals using DES [DES = 50% v/v ChCl:OA, time = 90 min, stirring speed = 250 rpm, and liquid-to-solid ratio = 1/10 (mL/g)].

Furthermore, higher temperatures are known to reduce the viscosity of the DES, facilitating improved mass transfer and enhanced diffusion of reactants into the solid matrix. These factors collectively account for the observed increase in leaching efficiencies with rising temperature. The temperature-dependent behaviour agrees with previous studies, which reported similar enhancements in metal extraction efficiencies using choline chloride-based DESs [43,45]. Overall, the data highlights the critical role of temperature in optimising the leaching process using ChCl:OA DES, indicating that careful thermal management can substantially improve the extraction of valuable metals from titanomagnetite ore.

3.4. Comparative Performance of the Investigated Methods

A comparison of the maximum recoveries achieved by roasting, ILs, and DESs under optimal conditions is presented in Table 2. These were synthesised based on the details

already discussed in Sections 3.1–3.3. Overall, DES leaching with ChCl:OA demonstrated the best performance, achieving the highest recoveries for both V (97.6%) and Ti (76.1%), with competitive Fe extraction (68.8%). The IL [Bmim][HSO_4] followed closely for V (95.6%) and offered higher Fe recovery (74.8%) than ChCl:OA, although Ti extraction was lower (53.2%). Roasting with Na_2CO_3 delivered high V recovery (86.5%) and moderate Ti and Fe extraction, whereas Na_2SO_4 roasting provided the best Fe yield (80.1%) but lower yields for V and Ti. The other IL ([Bmim][PF_6]) and DES (ChCl:SA) systems were clearly less effective, showing poor recoveries across all metals. These results underline a clear performance hierarchy: ChCl:OA > [Bmim][HSO_4] > Na_2CO_3 > Na_2SO_4 > ChCl:SA ≈ [Bmim][PF_6]. While DESs and ILs achieve comparable or superior recoveries at much lower temperatures than roasting, DESs also offer the advantages of biodegradability and cost-effectiveness, positioning them as the most promising option for sustainable metal recovery.

Table 2. Comparative performance of roasting, ILs, and DESs methods for V, Ti, and Fe recovery from titanomagnetite ore under optimal conditions.

Method	V LE (%)	Ti LE (%)	Fe LE (%)	Sustainability/Environmental Impact	Remarks
Roasting with Na_2CO_3	86.5	50.6	66.6	High energy demand; CO_2 emissions; sintering risk	Good V recovery; moderate Ti and Fe.
Roasting with Na_2SO_4	82.3	36.5	80.1	High temperature; sulphate residues	Best Fe recovery; weak for V and Ti.
[Bmim][HSO_4]	95.6	53.2	74.8	Low-temp operation; toxicity/recycling concerns	Excellent V; high Fe; Ti moderate.
[Bmim][PF_6]	31.3	19.1	27.9	Persistent; poor efficiency	Not viable.
ChCl:OA	97.6	76.1	68.8	Biodegradable, low-cost, low toxicity	Best overall recovery.
ChCl:SA	34.3	21.1	25.5	Greener than ILs, but poor yields	Inefficient.

3.5. Analysis of the Pre- and Post-Leached Titanomagnetite Ore

The XRD patterns of titanomagnetite ore before and after leaching with [Bmim][HSO_4] IL and ChCl:OA DES reveal clear evidence of phase evolution and selective dissolution (Figure 7). In the untreated sample, the diffractogram displays intense reflections corresponding to quartz (SiO_2) at ~24.4°, 31.1°, 32.6°, 39.4°, 50.4°, and 59.7° 2θ, with the 32.6° peak being dominant. Strong peaks are also observed for magnetite spinel phases near 30.1°, 35.5°, 43.2°, 57.2°, and 62.8°, consistent with Fe_3O_4/magnesioferrite. Chromite ($FeCr_2O_4$) contributes overlapping reflections at ~30.0°, 35.5°, and 62.6°, while vanadium-bearing phases such as Mg_2VO_4 are identified by reflections at ~18.7°, 29.4°, and 34.8°. In addition, Mg_2TiO_4 is detected through characteristic reflections around 33.1°, 35.6°, and 48.0°. Collectively, quartz and Fe-bearing spinels dominate the mineralogical assemblage. After leaching under optimised conditions ([Bmim][HSO_4], 50% *v*/*v*; T = 100 °C; t = 90 min; 250 rpm; L/S = 1/10 mL/g; ChCl:OA, 50% *v*/*v*; T = 100 °C; t = 90 min; 250 rpm; L/S = 1/10 mL/g), a pronounced decrease in the intensity of Mg_2VO_4 reflections at ~29.4° and 34.8° is observed, demonstrating preferential removal of vanadium-bearing phases. In contrast, the characteristic spinel peaks (30.1°, 35.5°, 43.2°) and Ti-bearing reflections (33.1°, 48.0°) remain relatively intense, confirming the limited dissolution of Fe- and Ti-oxides under the applied leaching regimes. The quartz reflections, particularly the dominant 32.6° peak, remain significantly unchanged, indicating its chemical inertness. Overall, the selective attenuation of vanadate peaks, coupled with the persistence of quartz and Fe–Ti oxide reflections, confirms that both [Bmim][HSO_4] IL and ChCl:OA DES act as effective lixiviants for V, while Fe and Ti-rich phases appear to be a little bit resistant to dissolution.

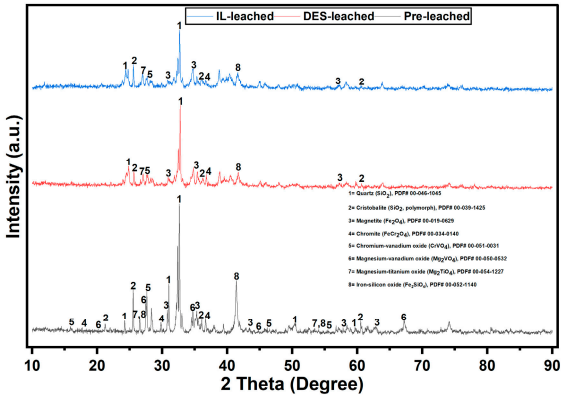


Figure 7. XRD patterns of the investigated pre- and post-leached titanomagnetite ore.

Furthermore, the disappearance of Mg_2VO_4 peaks in the XRD patterns of the residues after leaching indicates that vanadium dissolution proceeds through the breakdown of vanadate-bearing phases. In both [Bmim][HSO_4] and ChCl:OA, the acidic environment provides protons that promote this dissolution. Although no direct speciation analysis was performed, the acidic nature of the lixiviants used here makes the formation of anionic vanadate species such as VO_3^-, which dominate in alkaline solutions, highly unlikely [26]. Instead, vanadium is expected to occur predominantly as oxo-cationic species such as VO^{2+} (V^{4+}) and VO_2^+ (V^{5+}), and as oxalate complexes in the ChCl:OA system [61]. This interpretation is consistent with the attenuation of Mg_2VO_4 reflections in the XRD results. To further demonstrate that the pH of the leaching process is acid, the pH of 50% v/v [Bmim][HSO_4] and ChCl:OA aqueous solutions were determined at different temperatures (20 °C to 100 °C). The pH was measured using a calibrated benchtop pH meter (SKU: HI2210-01, Hanna Instruments, Woonsocket, RI, USA, ±0.01 pH accuracy) equipped with a HI1131B glass body pH electrode and a HI7662 temperature probe. The methodology used was according to the literature procedures for measuring aqueous DES solutions [62]. The temperature-dependent pH values for the 50% v/v ChCl:OA) solution DES and the 50% v/v solution were determined and are summarised in Table 3. The measurements confirmed that the leaching process operates under highly acidic conditions (pH < 3) across the entire tested temperature range, with the pH values decreasing further as temperature increases due to the enhanced dissociation of the HBD (oxalic acid) and the HSO_4^- anion, respectively.

Table 3. pH of 50% v/v aqueous solution of ChCl:OA and [Bmim][HSO_4] at different temperatures.

Temperature (°C)	ChCl:OA (50% v/v Aqueous) pH	[Bmim][HSO_4] (50% v/v Aqueous) pH
20	1.40	2.90
40	1.20	2.70
60	1.10	2.60
80	0.90	2.40
100	0.80	2.10

3.6. Kinetic Model of Leaching Process

Dissolution kinetics were investigated in a 50% (v/v) ChCl:OA solution over a temperature range of 20–100 °C and time intervals of 30–90 min, with stirring maintained at 250 rpm and a liquid-to-solid ratio of 10:1 mL/g. To determine the rate-controlling steps of the DES leaching process, the effect of leaching temperature and time on the dissolution of V, Ti, and Fe were examined, and the results are shown in Figure 8. For V (Figure 8a), the leaching efficiency increased markedly with temperature, rising from 27.5% at 20 °C

to 97.6% at 100 °C after 90 min, with equilibrium nearly reached within 75 min at higher temperatures. For Ti (Figure 8b), the efficiency improved from 25.0% at 20 °C to 76.1% at 100 °C after 90 min, although equilibrium was not achieved within the timeframe studied. For Fe (Figure 8c), the leaching efficiency was the lowest, increasing from 18.8% at 20 °C to 68.8% at 100 °C after 90 min, with equilibrium not attained even at the highest temperature. Overall, increasing temperatures significantly accelerated the dissolution of V, Ti, and Fe.

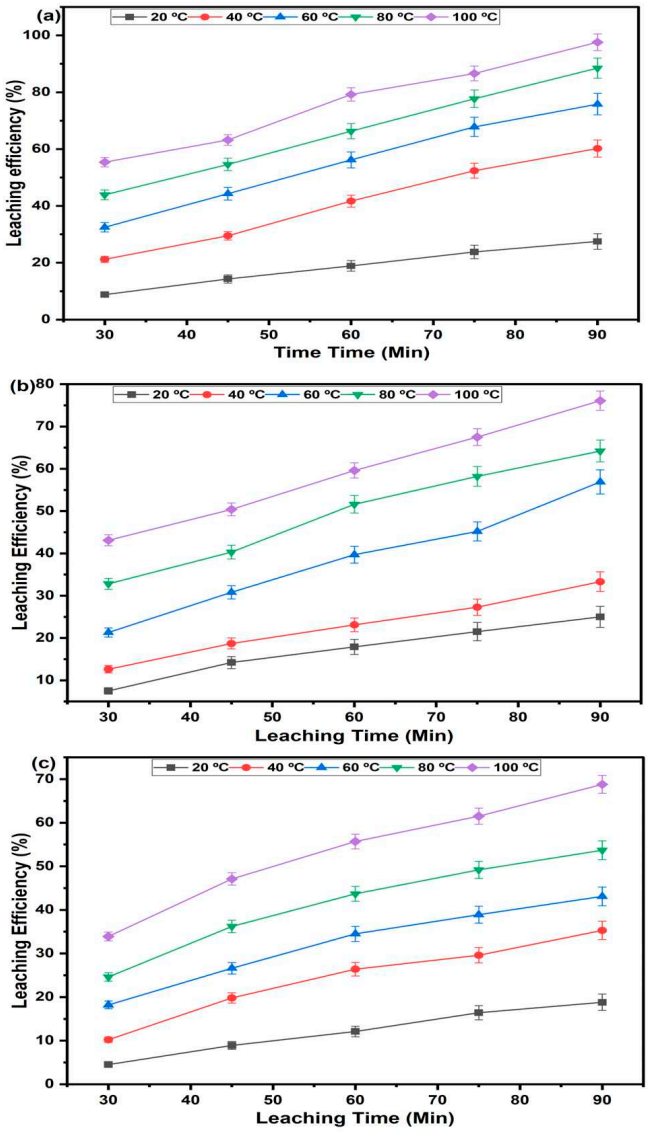


Figure 8. Relationship between leaching efficiency and leaching time at different temperatures for (**a**) V, (**b**) Ti, and (**c**) Fe.

The leaching kinetics were thereafter evaluated using shrinking core model (SCM). Consistent with previous studies, the SCM most accurately described the experimental data, displaying the highest correlation coefficient and confirming its suitability for representing the leaching process [63,64]. The leaching of V, Ti, and Fe can be classified as a typical liquid-solid two-phase reaction, in which the dissolution rate is either controlled by ion diffusion or by interfacial chemical reactions. To examine these possibilities, the SCM was applied to the leaching behaviour of the metals, considering both surface chemical

reaction control and diffusion through the product layer. The corresponding mathematical expressions are given in Equations (9) and (10) [63,64].

$$1 - (1 - x)^{\frac{1}{3}} = k_c t \quad (9)$$

$$1 - 3(1 - x)^{\frac{2}{3}} + 2(1 - x) = k_d t \quad (10)$$

In the above equations, x represents the leaching efficiency fraction of V, Ti and Fe, k_c and k_d are the apparent rate constants corresponding to the chemical reaction and diffusion-controlled processes, respectively, and t denotes the reaction time.

The apparent activation energy (E_a) of the leaching reaction serves as an important indicator for identifying the rate-controlling step and can be estimated by employing the Arrhenius equation, as shown in Equation (11).

$$\ln k = -\frac{Ea}{R}\left(\frac{1}{T}\right) + \ln A \quad (11)$$

In this case, k is the reaction rate constant, E_a is the apparent activation energy (kJ/mol), R is the gas constant (8.314 J/mol/K), T is the absolute temperature (K), and A is the pre-exponential factor.

The experimental data at different leaching temperatures were substituted into the above kinetic Equations (9) and (10). The scatter plots below were fitted using Microsoft Excel, and the results are shown in Figure S1a–c and Figure 9a–c for chemical and diffusion control models, respectively. The apparent rate constants (k_c and k_d) and correlation coefficients (R^2) at different temperatures were obtained and are presented in Table 4. The results demonstrate that the diffusion-controlled model provides a better linear fit than the surface chemical reaction model across all studied temperatures, with correlation coefficients closest to unity. This confirms that the leaching of V, Ti, and Fe from titanomagnetite ore using aqueous solution of ChCl:OA DES could be predominantly governed by diffusion through the product layer rather than by surface chemical reactions. Previous investigations have consistently shown that the dissolution behaviour of V, Ti, and Fe is predominantly governed by diffusion-controlled mechanisms [65–67]. These studies indicate that the rate at which these metals are leached from the mineral matrix is largely dictated by the transport of reactant species through the boundary layer surrounding the solid particles rather than by the intrinsic surface chemical reactions. The observations reported in these prior works align closely with our experimental results, providing further confirmation that diffusion plays a decisive role in controlling the leaching kinetics of V, Ti, and Fe. However, it should be noted that, while the diffusion-controlled SCM resulted in satisfactory fits for Fe and Ti, the V data exhibited poor. This likely reflects vanadium's complex surface and solution chemistry, including rapid complexation and transient speciation changes, which reduce the apparent linearity of the model. Alternative fit (mixed-control model) was tested but yielded poorer statistical performance and was therefore not reported.

To further elucidate the rate-controlling steps, the apparent activation energies for V, Ti, and Fe were calculated separately using the Arrhenius equation (Equation (11)). The slopes of the linear plots in Figure 10a–c, showing the relationship between lnk and 1/T during the leaching process, were used to calculate the activation energies, which were found to be 35.1 kJ/mol for V, 28.3 kJ/mol for Ti, and 29.8 kJ/mol for Fe. According to conventional kinetic theory, activation energies above 40 kJ/mol generally indicate surface chemical reaction control, whereas values less than 40 kJ/mol suggest that diffusion through the product layer is the rate-limiting step [59,68]. In agreement with this criterion, the calculated activation energies fall within the range. This conclusion is further supported by previously discussed kinetic modelling using SCM, which demonstrates that the diffusion-controlled

model provides a better linear fit than the surface chemical reaction model across all studied temperatures, with correlation coefficients closest to unity. Consequently, it can be concluded that the leaching of V, Ti, and Fe from titanomagnetite ore using aqueous ChCl:OA DES is predominantly governed by diffusion through the product layer rather than by interfacial chemical reactions.

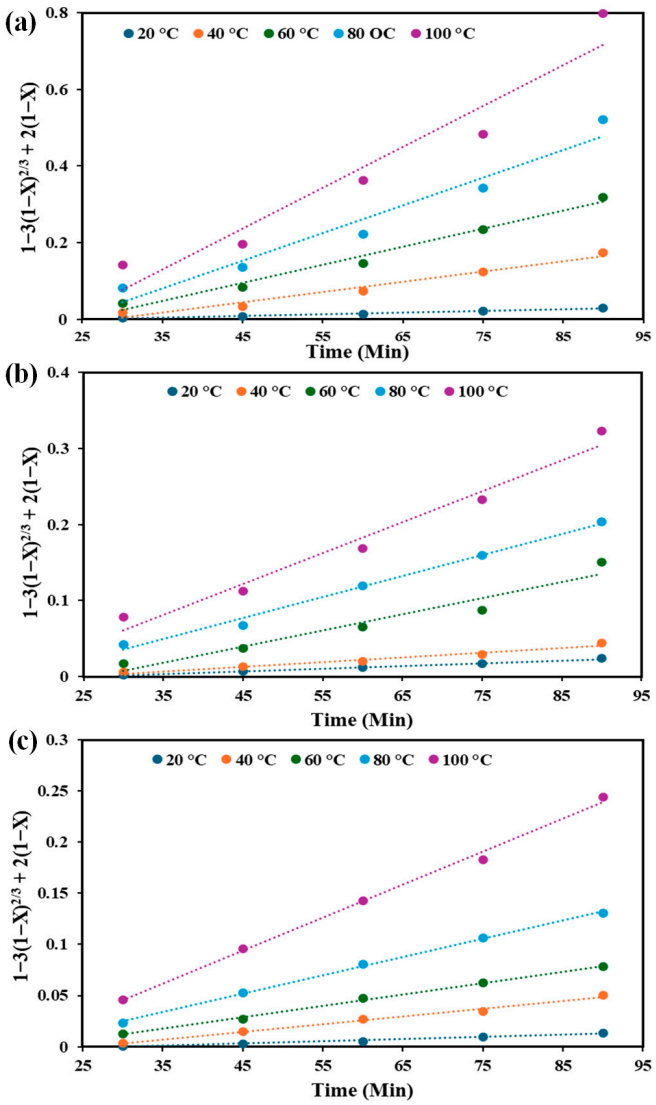


Figure 9. Relationship between $1-3(1-x)^{\frac{2}{3}}+2(1-x)$ (diffusion control model) and leaching time at different temperatures for (**a**) V, (**b**) Ti, and (**c**) Fe.

Table 4. The R^2 and k values of the leaching results at different temperatures using SCM.

V	$\mathbf{1-(1-x)^{\frac{1}{3}}}$ **(Chemical control)**		$\mathbf{1-3(1-x)^{\frac{2}{3}}+2(1-x)}$ **(Diffusion control)**	
T (°C)	$\mathbf{R^2}$	$\mathbf{k_c}$	$\mathbf{R^2}$	$\mathbf{k_d}$
20	0.9681	0.0012	0.9872	0.0004
40	0.9444	0.0032	0.9714	0.0027
60	0.9676	0.0043	0.9809	0.0047
80	0.9389	0.0056	0.9533	0.0072
100	0.9299	0.0077	0.9307	0.0107

Table 4. *Cont.*

Ti	$1-(1-x)^{\frac{1}{3}}$ (Chemical control)		$1-3(1-x)^{\frac{2}{3}}+2(1-x)$ (Diffusion control)	
T (°C)	**R^2**	**k_c**	**R^2**	**k_d**
20	0.9738	0.0011	0.9958	0.0004
40	0.9345	0.0013	0.9688	0.0006
60	0.9434	0.0027	0.9417	0.0021
80	0.9836	0.0028	0.9913	0.0028
100	0.9503	0.0035	0.9725	0.0041
Fe	$1-(1-x)^{\frac{1}{3}}$ (Chemical control)		$1-3(1-x)^{\frac{2}{3}}+2(1-x)$ (Diffusion control)	
T (°C)	**R^2**	**k_c**	**R^2**	**k_d**
20	0.9637	0.0009	0.9801	0.0002
40	0.9758	0.0016	0.9900	0.0007
60	0.9825	0.0018	0.9973	0.0011
80	0.9786	0.0022	0.9982	0.0018
100	0.9809	0.0031	0.9959	0.0032

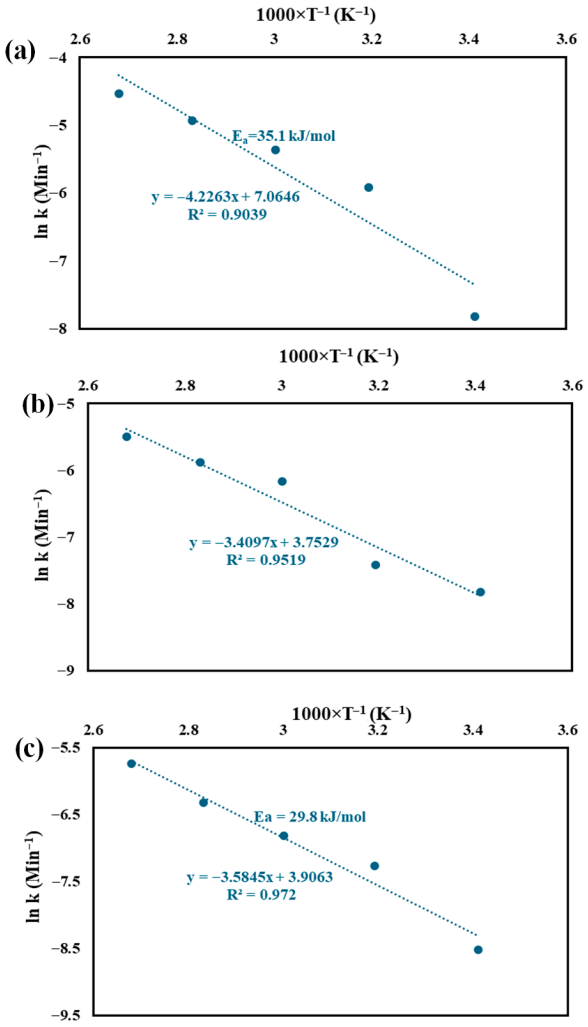


Figure 10. Relationship between lnk and 1/T during the leaching process of (**a**) V, (**b**) Ti, and (**c**) Fe.

4. Conclusions

This study demonstrates that ChCl:OA DES is the most effective and sustainable medium for extracting V, Ti, and Fe from South African titanomagnetite ore, achieving maximum recoveries of 97.6%, 76.1%, and 68.8%, respectively, under optimised conditions of 50% (v/v) and 100 °C. While [Bmim][HSO_4] also delivered high V and Fe recoveries, its performance for Ti was lower, and conventional salt roasting required high temperatures and significant energy input, highlighting environmental and operational limitations. Kinetic modelling confirms that the leaching process is diffusion-controlled, as reflected in apparent activation energies below 40 kJ/mol, and XRD analyses revealed V, Ti and Fe dissolution. Overall, ChCl:OA DES combines high extraction efficiency with biodegradability, low toxicity, and cost-effectiveness, positioning it as a promising green alternative for V recovery from titanomagnetite ores and providing valuable insights for sustainable metallurgical practices.

Supplementary Materials: The following supporting information can be downloaded at: https://www.mdpi.com/article/10.3390/separations12100285/s1, Figure S1: Relationship between $1-(1-x)^{\frac{1}{3}}$ (chemical control model) and leaching time at different temperatures for (a) V, (b) Ti, and (c) Fe.

Author Contributions: Conceptualisation, E.A.O., J.H.P. and L.D.v.D.; methodology, E.A.O., J.H.P. and L.D.v.D.; software, E.A.O.; formal analysis, D.N.; investigation, D.N.; resources, J.H.P.; data curation, E.A.O.; writing—original draft preparation, E.A.O. and D.N.; writing—review and editing, E.A.O. and J.H.P.; supervision, E.A.O., J.H.P. and L.D.v.D.; project administration, L.D.v.D. and J.H.P.; funding acquisition, J.H.P. All authors have read and agreed to the published version of the manuscript.

Funding: This research received no external funding.

Data Availability Statement: The original contributions presented in this study are included in the article/Supplementary Materials. Further inquiries can be directed to the corresponding author.

Acknowledgments: E.A.O. acknowledges the generous financial support provided to him by the Oppenheimer Memorial Trust (Grant Number: 2024-4758).

Conflicts of Interest: The authors declare no conflicts of interest.

Abbreviations

The following abbreviations are used in this manuscript:

ILs	Ionic liquids
DESs	Deep eutectic solvents
TOMAC	Tri-n-octylmethylammonium chloride
[BmimCF_3SO_3]	1-butyl-3-methylimidazolium trifluoromethane sulfonate
[BmimHSO_4]	1-butyl-3-methylimidazolium hydrogen sulphate
[Bmim][PF_6]	1-butyl-3-methylimidazolium hexafluorophosphate
ChCl	Choline chloride
HBA	Hydrogen bond acceptor
HBDs	Hydrogen bond donors
SA	Succinic acid
OA	Oxalic acid
XRF	X-ray fluorescence
XRD	X-ray diffraction
LE	Leaching efficiency
SCM	Shrinking core model
E_a	Apparent activation energy

References

1. Hu, P.; Zhang, Y.; Huang, J.; Liu, T.; Yuan, Y.; Xue, N. Eco-Friendly Leaching and Separation of Vanadium over Iron Impurity from Vanadium-Bearing Shale Using Oxalic Acid as a Leachant. *ACS Sustain. Chem. Eng.* **2018**, *6*, 1900–1908. [CrossRef]
2. Hu, P.; Zhang, Y.; Liu, T.; Huang, J.; Yuan, Y.; Xue, N. Source Separation of Vanadium over Iron from Roasted Vanadium-Bearing Shale during Acid Leaching via Ferric Fluoride Surface Coating. *J. Clean. Prod.* **2018**, *181*, 399–407. [CrossRef]
3. Zhang, Y.; Zhang, T.; Lv, G.; Zhang, G.; Liu, Y.; Zhang, W. Synergistic Extraction of Vanadium(IV) in Sulfuric Acid Media Using a Mixture of D2ehpa and Ehehpa. *Hydrometallurgy* **2016**, *166*, 87–93. [CrossRef]
4. Ibrahim, A.H.; Lyu, X.; Sharafeldin, H.E.; ElDeeb, A.B. Eco-Friendly and Complex Processing of Vanadium-Bearing Waste for Effective Extraction of Valuable Metals and Other By-Products: A Critical Review. *Recycling* **2025**, *10*, 6. [CrossRef]
5. Kelley, K.D.; Scott, C.; Polyak, D.E.; Kimball, B.E. *Vanadium*; Schulz, K.J., DeYoung, J.H., Seal, R.R., Bradley, D.C., Eds.; U.S. Geological Survey: Reston, VA, USA, 2017.
6. Yang, J.; Wang, Y.; Gao, X.; Zuo, R.; Song, L.; Jin, C.; Wang, J.; Teng, Y. Vanadium: A Review of Different Extraction Methods to Evaluate Bioavailability and Speciation. *Minerals* **2022**, *12*, 642. [CrossRef]
7. Luo, D.; Huang, J.; Zhang, Y.; Liu, H.; Hu, P. Highly Efficient Separation and Extraction of Vanadium from a Multi-Impurity Leachate of Vanadium Shale Using Tri-n-Octylmethylammonium Chloride. *Sep. Purif. Technol.* **2020**, *230*, 115842. [CrossRef]
8. Wang, Y.-H.; Wang, Y.-F.; Li, Y.-T.; Wu, C.; Han, X.-L.; Zhao, N.-N.; Zhang, Z.-K.; Dai, L.; Wang, L.; He, Z.-X. A Review on Vanadium Extraction Techniques from Major Vanadium-Containing Resources. *Rare Met.* **2024**, *43*, 4115–4131. [CrossRef]
9. Moskalyk, R.R.; Alfantazi, A.M. Processing of Vanadium: A Review. *Miner. Eng.* **2003**, *16*, 793–805. [CrossRef]
10. Zhang, Y.-M.; Bao, S.-X.; Liu, T.; Chen, T.-J.; Huang, J. The Technology of Extracting Vanadium from Stone Coal in China: History, Current Status and Future Prospects. *Hydrometallurgy* **2011**, *109*, 116–124. [CrossRef]
11. Li, C.; Jiang, T.; Wen, J.; Yu, T.; Li, F. Review of Leaching, Separation and Recovery of Vanadium from Roasted Products of Vanadium Slag. *Hydrometallurgy* **2024**, *226*, 106313. [CrossRef]
12. Han, C.; Li, L.; Yang, H.; Xue, X.-X. Preparation of V2O5 from Converter Slag Containing Vanadium. *Rare Met.* **2018**, *37*, 904–912. [CrossRef]
13. Langeslay, R.R.; Kaphan, D.M.; Marshall, C.L.; Stair, P.C.; Sattelberger, A.P.; Delferro, M. Catalytic Applications of Vanadium: A Mechanistic Perspective. *Chem. Rev.* **2019**, *119*, 2128–2191. [CrossRef]
14. Zeng, Y.K.; Zhao, T.S.; An, L.; Zhou, X.L.; Wei, L. A Comparative Study of All-Vanadium and Iron-Chromium Redox Flow Batteries for Large-Scale Energy Storage. *J. Power Sources* **2015**, *300*, 438–443. [CrossRef]
15. Wang, Z.; Qin, Z.; Chen, L.; Liang, B.; Zhu, Y.; Wu, K.; Luo, D. Recovery of Low Valence Vanadium from Vanadium Slag for the Preparation of VOSO4 Electrolyte. *Process Saf. Environ. Prot.* **2023**, *174*, 298–309. [CrossRef]
16. Nagata, M.; Matsuda, M.; Himeno, Y.; Shida, K.; Matsuda, M. Magnéli Phase Vanadium Oxide Thin Films Produced by Stepwise Oxidation of Vanadium Metal Foil. *Scr. Mater.* **2022**, *219*, 114884. [CrossRef]
17. Chen, Y.-S.; Ho, H.-C.; Lai, Y.-C.; Nagao, T.; Hsueh, C.-H. Thermochromic Vanadium Dioxide Film on Textured Silica Substrate for Smart Window with Enhanced Visible Transmittance and Tunable Infrared Radiation. *Infrared Phys. Technol.* **2019**, *102*, 103019. [CrossRef]
18. An, Y.; Ma, B.; Li, X.; Chen, Y.; Wang, C.; Wang, B.; Gao, M.; Feng, G. A Review on the Roasting-Assisted Leaching and Recovery of V from Vanadium Slag. *Process Saf. Environ. Prot.* **2023**, *173*, 263–276. [CrossRef]
19. Li, H.-Y.; Yang, Y.; Zhang, M.; Wei, W.; Xie, B. A Novel Anion Exchange Method Based on in Situ Selectively Reductive Desorption of Cr(VI) for Its Separation from V(V): Toward the Comprehensive Use of Hazardous Wastewater. *J. Hazard. Mater.* **2019**, *368*, 670–679. [CrossRef]
20. Ju, J.; Fu, H.-G.; Fu, D.-M.; Wei, S.-Z.; Sang, P.; Wu, Z.-W.; Tang, K.-Z.; Lei, Y.-P. Effects of Cr and V Additions on the Microstructure and Properties of High-Vanadium Wear-Resistant Alloy Steel. *Ironmak. Steelmak.* **2018**, *45*, 176–186. [CrossRef]
21. Dong, F.; Venezuela, J.; Li, H.; Shi, Z.; Zhou, Q.; Chen, L.; Chen, J.; Du, L.; Atrens, A. Effect of Vanadium and Rare Earth Microalloying on the Hydrogen Embrittlement Susceptibility of a Fe-18Mn-0.6C TWIP Steel Studied Using the Linearly Increasing Stress Test. *Corros. Sci.* **2021**, *185*, 109440. [CrossRef]
22. Gao, F.; Du, H.; Wang, S.; Chen, B.; Li, J.; Zhang, Y.; Li, M.; Liu, B.; Olayiwola, A.U. A Comparative Study of Extracting Vanadium from Vanadium Titano-Magnetite Ores: Calcium Salt Roasting Vs Sodium Salt Roasting. *Miner. Process. Extr. Metall. Rev.* **2023**, *44*, 352–364. [CrossRef]
23. Trinh, H.B.; Kim, S.; Lee, J.; Oh, S. Efficient Recovery of Vanadium and Titanium from Domestic Titanomagnetite Concentrate Using Molten Salt Roasting and Water Leaching. *Materials* **2023**, *16*, 6918. [CrossRef]
24. Bai, L.; Xiang, J.; Lu, X.; Xu, Y.; Zhu, K.; Yu, J.; Huang, Q.; Pei, G.; Lv, X. Extraction of Vanadium from Vanadium–Titanium Magnetite: Enhanced by Sodium–Calcium Synergistic Roasting–Water Leaching Process. *Metall. Mater. Trans. B* **2025**, *56*, 552–563. [CrossRef]
25. Petranikova, M.; Tkaczyk, A.H.; Bartl, A.; Amato, A.; Lapkovskis, V.; Tunsu, C. Vanadium Sustainability in the Context of Innovative Recycling and Sourcing Development. *Waste Manag.* **2020**, *113*, 521–544. [CrossRef]

26. Gao, F.; Olayiwola, A.U.; Liu, B.; Wang, S.; Du, H.; Li, J.; Wang, X.; Chen, D.; Zhang, Y. Review of Vanadium Production Part I: Primary Resources. *Miner. Process. Extr. Metall. Rev.* **2022**, *43*, 466–488. [CrossRef]
27. Chen, B.; Jiang, T.; Wen, J.; Yang, G.; Yu, T.; Zhu, F.; Hu, P. High-Chromium Vanadium–Titanium Magnetite All-Pellet Integrated Burden Optimization and Softening–Melting Behavior Based on Flux Pellets. *Int. J. Miner. Metall. Mater.* **2024**, *31*, 498–507. [CrossRef]
28. Sun, H.; Adetoro, A.A.; Wang, Z.; Zhu, Q. Behavior and Mechanism of Pre-Oxidation Improvement on Fluidization in the Fluidized Reduction of Titanomagnetite. *Int. J. Miner. Metall. Mater.* **2024**, *31*, 2458–2465. [CrossRef]
29. Li, S.; Zhang, Y.; Yuan, Y.; Hu, P. An Insight on the Mechanism of Efficient Leaching of Vanadium from Vanadium Shale Induced by Microwave-Generated Hot Spots. *Int. J. Miner. Metall. Mater.* **2023**, *30*, 293–302. [CrossRef]
30. Dong, Y.; Chong, S.; Lin, H. Bioleaching and Biosorption Behavior of Vanadium-Bearing Stone Coal by Bacillus Mucilaginosus. *Int. J. Miner. Metall. Mater.* **2023**, *30*, 283–292. [CrossRef]
31. Dong, Y.; Zan, J.; Lin, H. Bioleaching of Vanadium from Stone Coal Vanadium Ore by Bacillus Mucilaginosus: Influencing Factors and Mechanism. *Int. J. Miner. Metall. Mater.* **2024**, *31*, 1828–1838. [CrossRef]
32. Tian, G.; Liu, H. Review on the Mineral Processing in Ionic Liquids and Deep Eutectic Solvents. *Miner. Process. Extr. Metall. Rev.* **2024**, *45*, 130–153. [CrossRef]
33. Al-Bodour, A.; Alomari, N.; Perez-Duran, G.; Rozas, S.; Iglesias-Silva, G.; Aparicio, S.; Gutierrez-Vega, A.; Atilhan, M. Ionic Liquids as Multidimensional Materials: A Review from Fundamentals to Applications. *Energy Fuels* **2025**, *39*, 12791–12829. [CrossRef]
34. Lei, Z.; Dai, C.; Hallett, J.; Shiflett, M. Introduction: Ionic Liquids for Diverse Applications. *Chem. Rev.* **2024**, *124*, 7533–7535. [CrossRef]
35. Yu, Z.; Liu, T.; Zhang, Y.; Hu, P.; Liu, H.; He, Y. Mechanism of Selectivity of Tri-n-Octylmethylammonium Chloride for Vanadium. *Miner. Eng.* **2024**, *218*, 109052. [CrossRef]
36. Potgieter, H.; Teimouri, S. Investigation into the Possibility of Using a Novel Ionic Liquid Leaching Method to Obtain Vanadium from Vanadium Slag. *Environ. Res. Technol.* **2023**, *6*, 1–7. [CrossRef]
37. Yu, Z.; Liu, T.; Zhang, Y.; Hu, P. Optimizing Vanadium Extraction from Shale Leachate Using Salicylhydroxamic Acid-Tri-n-Octylmethylammonium. *J. Clean. Prod.* **2025**, *496*, 145144. [CrossRef]
38. Abbott, A.P.; Boothby, D.; Capper, G.; Davies, D.L.; Rasheed, R.K. Deep Eutectic Solvents Formed between Choline Chloride and Carboxylic Acids: Versatile Alternatives to Ionic Liquids. *J. Am. Chem. Soc.* **2004**, *126*, 9142–9147. [CrossRef]
39. Oke, E.A.; Potgieter, H. Recent Chemical Methods for Metals Recovery from Printed Circuit Boards: A Review. *J. Mater. Cycles Waste Manag.* **2024**, *26*, 1349–1368. [CrossRef]
40. Oke, E.A.; Potgieter, J.H. Sustainable Leaching of Metals from Waste Printed Circuit Boards Using Efficient Carboxylic Acid-Based Deep Eutectic Solvents. *Sep. Purif. Technol.* **2025**, *374*, 133712. [CrossRef]
41. Hansen, B.B.; Spittle, S.; Chen, B.; Poe, D.; Zhang, Y.; Klein, J.M.; Horton, A.; Adhikari, L.; Zelovich, T.; Doherty, B.W.; et al. Deep Eutectic Solvents: A Review of Fundamentals and Applications. *Chem. Rev.* **2021**, *121*, 1232–1285. [CrossRef]
42. Surauzhanov, K.; Ultarakova, A. Extraction of Vanadium from the Dust of Ore-Thermal Melting of Ilmenite Concentrate Using Deep Eutectic Solvents. *Chem. Eng. Trans.* **2021**, *88*, 1015–1020. [CrossRef]
43. Chen, S.-C.; Chou, F.-C.; Shirke, S.; Lin, S.-Y.; Lin, Y.-C. Efficiency Comparison of Succinic Acid and Oxalic Acid with Choline Chloride Deep-Eutectic Solvent through Response Surface Methodology. *J. Taiwan Inst. Chem. Eng.* **2025**, *174*, 106230. [CrossRef]
44. Li, T.; Xiong, Y.; Yan, X.; Hu, T.; Jing, S.; Wang, Z.; Ge, X. Closed-Loop Cobalt Recycling from Spent Lithium-Ion Batteries Based on a Deep Eutectic Solvent (DES) with Easy Solvent Recovery. *J. Energy Chem.* **2022**, *72*, 532–538. [CrossRef]
45. Oke, E.A.; Fedai, Y.; Potgieter, J.H. Hydrometallurgical Leaching of Copper and Cobalt from a Copper–Cobalt Ore by Aqueous Choline Chloride-Based Deep Eutectic Solvent Solutions. *Minerals* **2025**, *15*, 815. [CrossRef]
46. Tan, J.; Huang, R.; Li, K.; Yan, X.; Guo, L.; Guo, Z.; Zhang, W.; Chai, L. Achieving High Solid–Liquid Ratio through Competitive Coordination towards Efficient Recovery of Metals from Spent Batteries. *Angew. Chem.* **2025**, *137*, e202422313. [CrossRef]
47. Septioga, K.; Fajar, A.T.N.; Wakabayashi, R.; Goto, M. Deep Eutectic Solvent-Aqueous Two-Phase Leaching System for Direct Separation of Lithium and Critical Metals. *ACS Sustain. Resour. Manag.* **2024**, *1*, 2482–2491. [CrossRef]
48. Nkosi, S.B.; Goso, X.C.; Mokone, T.; Petersen, J. Preliminary investigations into the extraction of vanadium from titaniferous slags using a modified vanadium primary production process. In Proceedings of the Hydrometallurgy for the Future, Stellenbosch, South Africa, 3–9 September 2024.
49. Xu, S.; Long, M.; Li, Y.; Chen, D.; Fan, H.; Zhao, Y.; Ma, Y. Study on Roasting Parameters for Extraction of Vanadium from a High Ca/V Ratio Vanadium Slag. *Metal. Int.* **2013**, *18*, 38.
50. Gilligan, R.; Nikoloski, A.N. The Extraction of Vanadium from Titanomagnetites and Other Sources. *Miner. Eng.* **2020**, *146*, 106106. [CrossRef]
51. Wang, B.; Yang, Q. Optimization of Roasting Parameters for Recovery of Vanadium and Tungsten from Spent SCR Catalyst with Composite Roasting. *Processes* **2021**, *9*, 1923. [CrossRef]

52. Zhou, Z.; Jin, J.; Zhu, Y.; Han, Y.; Bai, Z.; Tang, Z. Effect of Roasting Temperature on Vanadium Extraction, Kinetics, Phase Transformation, and Microstructure Evolution of Vanadium-Bearing Shale during Suspension Oxidation Roasting Process. *Adv. Powder Technol.* **2023**, *34*, 104233. [CrossRef]
53. Kuzmina, O.; Symianakis, E.; Godfrey, D.; Albrecht, T.; Welton, T. Ionic Liquids for Metal Extraction from Chalcopyrite: Solid, Liquid and Gas Phase Studies. *Phys. Chem. Chem. Phys.* **2017**, *19*, 21556–21564. [CrossRef] [PubMed]
54. Dong, T.; Hua, Y.; Zhang, Q.; Zhou, D. Leaching of Chalcopyrite with Brønsted Acidic Ionic Liquid. *Hydrometallurgy* **2009**, *99*, 33–38. [CrossRef]
55. Rodríguez, M.; Ayala, L.; Robles, P.; Sepúlveda, R.; Torres, D.; Carrillo-Pedroza, F.R.; Jeldres, R.I.; Toro, N. Leaching Chalcopyrite with an Imidazolium-Based Ionic Liquid and Bromide. *Metals* **2020**, *10*, 183. [CrossRef]
56. Oke, E.A.; Potgieter, H.; Mondlane, F.; Skosana, N.P.; Teimouri, S.; Nyembwe, J.K. Concurrent Leaching of Copper and Cobalt from a Copper–Cobalt Ore Using Sulfuric and Organic Acids. *Miner. Eng.* **2024**, *216*, 108853. [CrossRef]
57. Wang, Z.; Peng, Z.; Li, Y.; Zhu, Y.; Xie, K. Selective Sulfuric Acid Cyclic Leaching of Vanadium from the Calcification Roasting Pellets of Vanadium Titanomagnetite. *J. Mater. Res. Technol.* **2023**, *23*, 778–790. [CrossRef]
58. Pateli, I.M.; Thompson, D.; Alabdullah, S.S.M.; Abbott, A.P.; Jenkin, G.R.T.; Hartley, J.M. The Effect of PH and Hydrogen Bond Donor on the Dissolution of Metal Oxides in Deep Eutectic Solvents. *Green Chem.* **2020**, *22*, 5476–5486. [CrossRef]
59. Olaoluwa, D.T.; Baba, A.A.; Oyewole, A.L. Beneficiation of a Nigerian Lepidolite Ore by Sulfuric Acid Leaching. *Miner. Process. Extr. Metall.* **2023**, *132*, 134–140. [CrossRef]
60. Oke, E.A.; Potgieter, J.H. Effectiveness of Acidic Deep Eutectic Solvents in Recovery of Hazardous Base Metals from Waste Printed Circuit Boards. *Environ. Sci. Pollut. Res.* **2025**, *32*, 16361–16379. [CrossRef]
61. Cheng, W.; Li, J.; Deng, J.; Li, Y.; Cheng, F. Leaching Vanadium from the Spent Denitration Catalyst in the Sulfuric Acid/Oxalic Acid Combined Solvent. *ACS Omega* **2024**, *9*, 9286–9294. [CrossRef]
62. Skulcova, A.; Russ, A.; Jablonsky, M.; Sima, J. The PH Behavior of Seventeen Deep Eutectic Solvents. *Bioresources* **2018**, *13*, 5042–5051. [CrossRef]
63. Wang, Z.; Li, Z.; Chen, L.; Zhu, Y.; Wu, K.; Luo, D. Optimization and Kinetic Analysis of Co-Extraction of Vanadium(IV) and Chromium(III) from High Chromium Vanadium Slag with Titanium Dioxide Waste Acid. *Miner. Eng.* **2025**, *233*, 109604. [CrossRef]
64. Cheng, J.; Li, H.; Hai, D.; Chen, X.; Diao, J.; Xie, B. Acidic Leaching Kinetics Study on Vanadium from Magnesiation-Roasted Vanadium Slag. *Trans. Nonferrous Met. Soc. China* **2024**, *34*, 669–680. [CrossRef]
65. Lin, Y.; Sun, H.; Peng, T.; Zhao, D.; Zhang, X. The Leaching Kinetics of Iron from Titanium Gypsum in a Citric Acid Medium and Obtain Materials by Leaching Liquid. *Molecules* **2023**, *28*, 952. [CrossRef]
66. Gao, L.; Rao, B.; Dai, H.; Xie, H.; Wang, P.; Ma, F. Kinetics of Sulphuric Acid Leaching of Titanium from Refractory Anatase under Atmospheric Pressure. *Physicochem. Probl. Miner. Process.* **2019**, *55*, 467–478. [CrossRef]
67. Peng, H.; Shang, Q.; Chen, R.; Leng, Y.; Guo, J.; Liu, Z.; Tao, C. Oxidative Leaching Kinetics of Vanadium from the Vanadium-Chromium-Reducing Residue with $K_2Cr_2O_7$. *ACS Omega* **2020**, *5*, 8777–8783. [CrossRef]
68. Salem, A.R. Efficient Leaching Process of Valuable Elements from Gibbsite Ore Materials in Talet Seleim, Southwestern, Sinai, Egypt Using Green and Ecofriendly Lixiviant Agent: Optimization, Kinetic and Thermodynamic Study. *Anal. Chem. Lett.* **2023**, *13*, 141–158. [CrossRef]

Disclaimer/Publisher's Note: The statements, opinions and data contained in all publications are solely those of the individual author(s) and contributor(s) and not of MDPI and/or the editor(s). MDPI and/or the editor(s) disclaim responsibility for any injury to people or property resulting from any ideas, methods, instructions or products referred to in the content.